V. Ivanov and *J. Bousquet*

Assessing reactor physics codes capabilities to simulate fast reactors on the example of the BN-600 Benchmark

This work aims to assess the capabilities of reactor physics codes (initially validated for thermal reactors) to simulate fast sodium cooled reactors. The BFS-62-3A critical experiment from the BN-600 Hybrid Core Benchmark Analyses was chosen for the investigation. Monte-Carlo codes (KENO from SCALE and SERPENT 2.1.23) and the deterministic diffusion code DYN3D-MG are applied to calculate the neutronic parameters. It was found that the multiplication factor and reactivity effects calculated by KENO and SERPENT using the ENDF/B-VII.0 continuous energy library are in a good agreement with each other and with the measured benchmark values. Few-groups macroscopic cross sections, required for DYN3D-MG, were prepared in applying different methods implemented in SCALE and SERPENT. The DYN3D-MG results of a simplified benchmark show reasonable agreement with results from Monte-Carlo calculations and measured values. The former results are used to justify DYN3D-MG implementation for sodium cooled fast reactors coupled deterministic analysis.

Untersuchung der Berechnung schneller Reaktoren mit reaktorphysikalischen Programmen am Beispiel des BN-600 Benchmarks. *Dieser Beitrag untersucht die Anwendbarkeit von reaktorphysikalischen Programmen, die für thermische Reaktoren validiert sind, für schnelle Natriumgekühlte Reaktoren. Dazu wurde das Experiment BFS-62-3A der BN-600 Hybrid-Core Benchmarkanalysen ausgewählt und nachgerechnet. Dazu wurden Rechnungen mit den Monte-Carlo-Codes KENO von SCALE und SERPENT 2.1.23 und dem deterministischen Diffusionsprogramm DYN3D-MG durchgeführt und die Ergebnisse verglichen. Es zeigte sich, dass der Multiplikationsfaktor und die Reaktivitätseffekte, die mit KENO und SERPENT unter zur Hilfenahme der ENDF / B-VII.0 Bibliothek gut untereinander und gut mit den Messwerten übereinstimmen. Für die Berechnungen mit DYN3D-MG müssen Gruppen makroskopischer Querschnitte vorab berechnet werden. Diese Daten wurden mit SCALE und SERPENT unter Anwendung unterschiedlicher Methoden, bestimmt. Die damit durchgeführten DYN3D-MG Ergebnisse eines vereinfachten Benchmarks zeigten eine gute Übereinstimmung mit den Ergebnissen der Monte-Carlo-Rechnungen und mit den Messwerten. Aus diesen Ergebnissen wird abgeleitet, dass Anwendung von DYN3D-MG bei natriumgekühlten schnellen Reaktoren möglich ist.*

1 Introduction

Several liquid metal-cooled fast reactor projects are under development (ASTRID, MYRRHA, ALFRED, BN-800, BREST-300, SVBR-100 etc.). Therefore it is important to perform independent safety assessments of such systems. The main goal of this work is to check the capabilities of SCALE [2], SERPENT [3] and DYN3D [4] reactor physics codes, which are originally validated for thermal reactors [3, 5], to simulate fast reactors.

The BFS-62-3A critical experiment from the BN-600 Hybrid Core Benchmark Analyses was chosen for the study [1]. The benchmark was designed to simulate BN-600 hybrid modified core project. The main difference from the operating BN-600 core is the significant amount of MOX fuel and an axial steel reflector. In the experiment, several neutron physic characteristics were measured: effective multiplication factor, control and safety rods weight, axial and radial reaction rate distributions, and Sodium Void Reactivity Effect (SVRE).

A two-step approach was used for the benchmark analysis. The first step included the comparison of Monte-Carlo codes (KENO-VI from SCALE6.0 and SERPENT 2.1.23) using the continuous energy cross sections based on ENDF/B-VII.0 evaluated data. The "as build" model with minor simplifications was used for Monte-Carlo calculations. The second step aimed to assess the effect of model and method simplification. The deterministic DYN3D-MG code was used to calculate the "simplified" benchmark core with homogenized elements. SCALE and SERPENT codes were used to produce problem depended few-groups macroscopic cross-sections. Different methods of cross section processing and collapsing were tested. In order to evaluate the effect of model simplification on DYN3D-MG results, Monte-Carlo calculation results obtained with SERPENT and KENO were used.

2 Description of the referenced benchmark core

The BFS-62-3A is a part of series of critical experiments conducted by the Russian Institute of Physics and Power Engineering (IPPE) in support to the disposal of Russian surplus weapons plutonium in the commercial fast reactor BN-600. The benchmark is a representation of BN-600 hybrid core with about 20 % of uranium fuel rods replaced by MOX fuel rods (Fig. 1). Each subassembly is composed of one steel tube surrounded by 6 stainless steel sticks arranged within a hexagonal lattice with a pitch of 5.1 cm. Each tube is axially composed of fuel and structural material pellets with a diameter of 4.7 cm. There are three fueled regions in the core: Inner Core (IC), Middle Core (MC) and Outer Core (OC), consisting of UO2 fuel with different enrichments. The core layout is shown in the Fig. 2. The core is surrounded by radial and axial blankets consisting of depleted uranium dioxide. Moreover, a 120° sector of the radial blanket outside the core has been replaced by stainless steel, with naturally enriched boron carbide being located behind this sector. Also different sodium pellets were used in the 120° sector of fuel zones. The old ones, so called "green pellets", containing some amount of hydrogen, are outside. The new ones, so called "laser pellets", free of hydrogen, are inside the 120° sector. A MOX fueled zone has been added like a ring between the Middle Core and Outer Core zones. Six control rods and six safety rods mock-ups are located in the inner zone. Twelve other control rods are located between inner and middle core. Fuel zones are axially surrounded with blanket and steel reflector.

3 Precise modeling with Monte-Carlo

3.1 Multiplication factor

The critical calculation results are shown in the Table 1. The results obtained with MMKKENO and MCNP from ref. [6, 7] were listed for comparison. The reactivity effects and multiplication factor are in a good agreement with experimental data. According to ref. [7], several MCNP5 calculations using different nuclear libraries (ENDF/B-VII.0, ENDF/B-VII.1, JEFF-3.1.1, BROND-3, JENDL-3.3) were performed. The overall comparison of Monte-Carlo calculations shows that the differences in continuous energy cross sections affect critical calculations less than the uncertainty in input data. The total modeling uncertainty effect on critical calculations was studied by IPPE [1] and appeared to be around 300 pcm for the multiplication factor. The amount of Monte-Carlo neu-

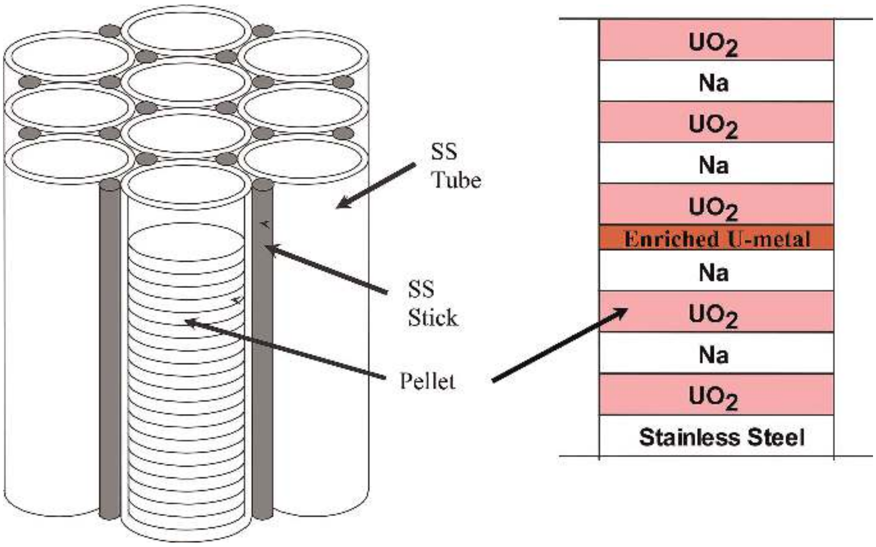

Fig. 1. Example structure of BFS subassembly

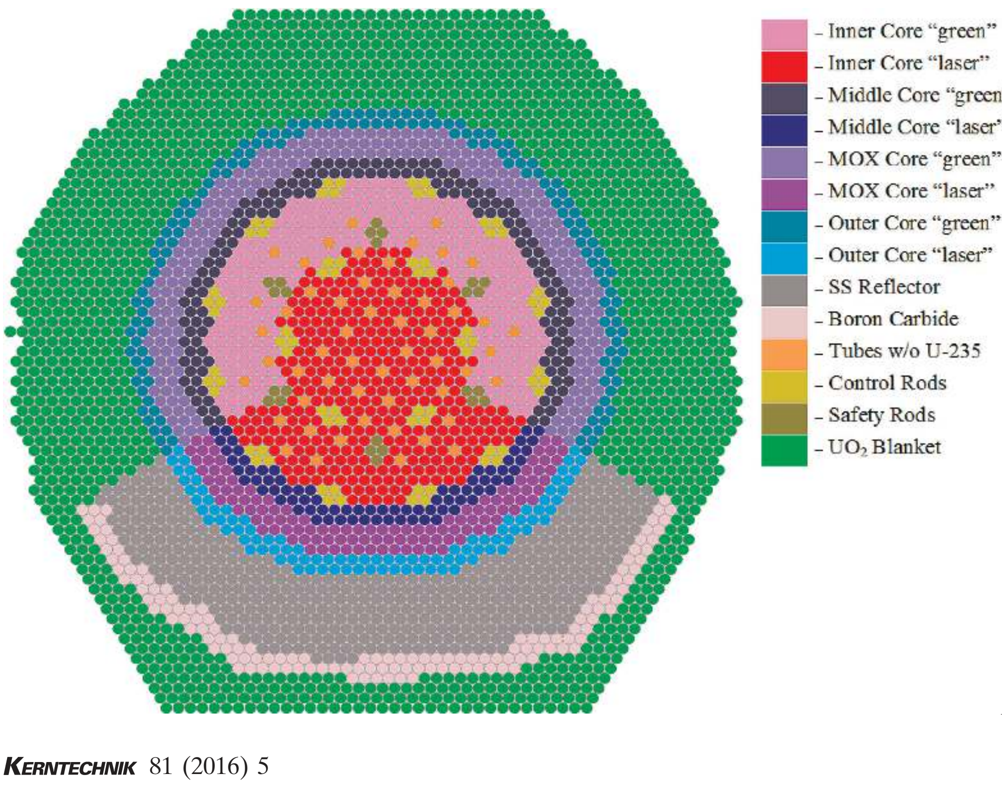

Fig. 2. BFS-62-3A core layout

tron histories were chosen to obtain less than 5 pcm deviation for multiplication factor (200 million neutron histories were used in KENO, 300 million in SERPENT).

As far as KENO and SERPENT critical calculations are in a good agreement (same input data was used for both codes), it may be assumed that continuous energy cross section processing in both codes are consistent for the referenced benchmark problem. Difference with MCNP is approximately in range of input data uncertainty calculated by IPPE. The difference with measured value is around 100 pcm which is in agreement with MCNP and MMKKENO calculations.

3.2 Control and Safety rods worth

The control and safety rods worth was calculated with KENO for further validation of ENDF/B 7.0 continuous energy library. The Table 2 shows the results obtained. In the BFS-62-3A experiment, five control rod and two safety rod mock-ups were inserted in the core, only one at a time, leading to core reactivity reductions between 45 and 95 cents, depending on the position of the inserted control/safety rod. The value of $\beta_{eff} = 0.00617$ from [6] was used to convert benchmark values of rod weights and SVRE in pcm.

3.3 Sodium Void Reactivity Effect

The BFS-62-3A experiment included an analysis of SVRE. In particular, sub-zones of the four core regions containing “laser” Na pellets were separately voided. The corresponding effects on the effective multiplication factor were measured. The sodium void effect is experimentally negative for all the four regions and simulations are in quantitative agreement. The Table 3 summarizes the measured values and results.

Table 1. Calculated multiplication factors and comparison to measured value

	Library used	Multiplication factor	Deviation from measured value, pcm
Measured value		1.0007 ± 0.003	
KENO	ENDF/B-VII.0	1.0014	72
SERPENT	ENDF/B-VII.0	0.9997	–101
MCNP5	ENDF/B-VII.0	1.0069	615
MCNP5	ENDF/B-VII.1	1.0059	516
MCNP5	JEFF-3.1.1	1.0068	605
MCNP5	BROND-3	1.0053	457
MCNP5	JENDL-3.3	0.9993	140
MMKKENO	ABBN-93	1.0018	109

Table 2. Calculated control and safety rods weights [pcm]

	KENO (SCALE6.0)	MMKKENO	MCNP5	Measured value
CR 1-3	–27	–36	–	–34 ± 1
CR 1-6	–36	–34	–36	–34 ± 1
CR 3-5	–23	–29	–	–28 ± 1
CR3-11	–33	–28	–	–28 ± 1
SR 2-2	–45	–56	–62	–59 ± 2
SR 2-5	–67	–55	–	–54 ± 2

Table 3. Calculated SVRE [pcm]

	KENO (SCALE6.0)	MMKKENO	MCNP5	Measured value
Inner core	–36	–73	–	–57 ± 3
Middle core	–13	–19	2	–15 ± 2
Outer core	–43	–48	–38	–32 ± 2
MOX core	–71	–33	–60	–71 ± 3

4 Model simplifications for deterministic analysis

4.1 Simplified model

In the "simplified model" appropriate for deterministic methods, the rod structure is represented as a single homogeneous cell. The simplified model geometry is described in accordance with IAEA homogeneous BFS-62-3A benchmark [8] but homogenized material compositions were calculated in accordance with full scale Monte-Carlo model. Every steel tube with corresponding pellet composition and surrounding dowels is homogenized in hexagonal shape with 5.1 cm pitch. The axial dimensions are adjusted in order to fix the same height for every assembly element (fuel zones; blankets; stainless steel shield and support layer, see Fig. 3). The bottom part of the support layer, grid plate and upper part of the tubes are removed.

4.2 Cross sections processing methods

Results obtained with deterministic methods are significantly affected by few-group cross section processing methods. The difference between homogeneous and heterogeneous critical calculations (heterogeneous effect) also affects the results. To reduce the heterogeneous and group structure effects, problem dependent cross section libraries are required. The first way is to prepare homogenized isotopic composition for corresponding cross sections processing (**homogeneous cross sections**). The 2-D neutron code NEWT (SCALE) was used to collapse SCALE 238-group ENDF/B-VII.0 library into 28 groups and to prepare homogeneous macroscopic cross sections. To perform resonance corrections continuous energy spectrum is used. Another cross sections set was prepared with SERPENT by collapsing continuous energy ENDF/B-VII.0 library.

The second way (performed only with NEWT) is to prepare cross sections for the heterogeneous case and to homogenize these cross sections using a weighting function (**homogenized weighted cross sections**). This method assures preservation of reaction rates in homogenized model which reduces the heterogeneous effect.

4.2.1 Homogeneous cross sections processing

For every type of assembly's axial section, the homogenized isotopic composition is treated with the homogenized infinite medium method and "smeared" into a single homogenized

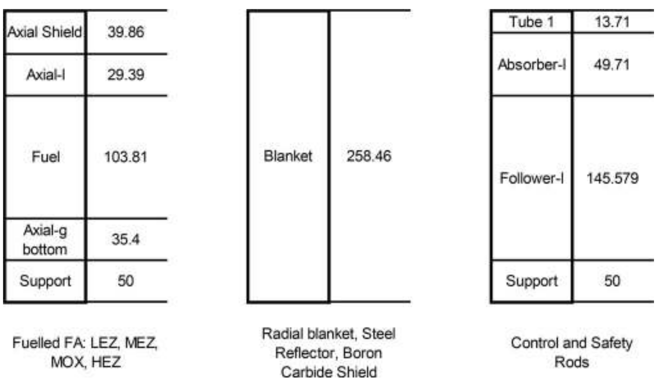

Fig. 3. Vertical compositions (in cm) of homogenized Fuel, reflector and control/safety Assemblies

mixture using number densities as a weighting function. In this method, the "zero-dimensional" model, which has no spatial or angular flux variation, is used. The calculated flux is used for resonance self-shielding processing. It is also necessary to collapse the homogenized group data into a reasonable amount of groups. An infinite model was used in NEWT to calculate cross sections set. The calculated spectrum was used for collapsing the cross sections into a 28 energy-group structure. This energy grid (Table 4) is based on the ABBN-93 28-group library grid [9].

Another homogeneous cross sections set was prepared with the SERPENT code. The calculation method is similar to SCALE. The main difference is that ENDF/B-VII.0 continuous energy library was used. For the preparation of the macroscopic cross sections library, it was decided to use an 8-group energy structure based on an ERANOS code energy grid [10]. Indeed, DYN3D-MG calculations, published in ref. [11], performed with a 33-group cross section library prepared by SERPENT, shows very large statistical errors in the thermal flux, due to the very low number of tally scores.

The resulting cross sections are meant to represent pure homogenized calculations. No correction was considered for the heterogeneity of the full scale model structure. Therefore the resonance shielding between pellets in the tubes is not taken into account. Only the resonance self-shielding is included. These cross section sets are applicable for heterogeneous effect calculation.

4.2.2 Homogenized weighted cross section processing

To provide a resonance-corrected cross section library based on the physical characteristics of the problem, an equivalent one-dimensional model was used for problem dependent point-wise flux calculation.

BFS-62-3A assembly axial sections may be represented as parallel layers. Every pellet is homogenized in hexagonal shape including tube, void and dowels (Fig. 4). For every type of fuel containing zones (IC, MC, OC, MOX) such 1-dimensional infinite layer model was used for cross section processing.

The two-dimensional lattice code NEWT was applied to collapse 238-group problem depended libraries. The collapsed 28-group energy grid from Table 4 was used. NEWT was also used to produce macroscopic weighted cross sections of layers homogenized into one mixture. Such homogenization is needed to match the problem depended library with the simplifyed model geometry. Homogenized cross sections were created using the 28-group energy structure. The flux weighted collapsed microscopic cross sections were combined with number densities in every layer and added such that reaction rates in homogenized material were conserved. The cross sections prepared in this way are meant to be more applicable for complex geometry representation.

5 Results and comparisons

5.1 Multiplication factor

The homogeneous model was implemented for DYN3D-MG, KENO and SERPENT. Table 5 shows the results obtained with homogeneous cross section libraries sets. Both 28-group and 8-group libraries were used for DYN3D-MG calculations. Monte-Carlo calculations used continuous energy libraries for the analysis. A difference is observed in the multiplication factor calculated by KENO (SCALE) and SERPENT codes in the range of 290 pcm (170 pcm for heterogeneous calculations respectively).

Due to the fact that homogeneous cross section sets were applied, it was possible to compare the Monte-Carlo multiplication factors with DYN3D-MG results.

The difference between multiplication factors calculated by DYN3D-MG with cross sections prepared by SCALE and SERPENT is 278 pcm. It is shown that the cross sections calculated by Serpent and NEWT are consistent to continuous energy Monte-Carlo simulations. Overall difference between DYN3D-MG and Monte-Carlo codes is 205 and 363 pcm for SERPENT and SCALE. Cross sections generated by SERPENT appear to be more correct due to the application of continuous energy library for their processing.

Table 6 shows the results obtained with homogenized weighted cross section set. Multiplication factors obtained with these cross sections compare reasonably with heterogeneous model results.

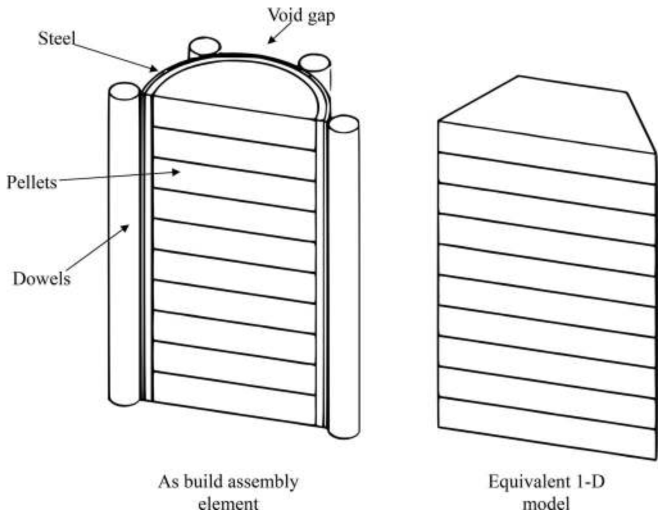

Fig. 4. Equivalent 1-D model

Table 4. Fine group energy structure

28-group energy grid based on ABBN-93			
Upper energy [eV]	Group number	Upper energy [eV]	Group number
$20.00 \cdot 10^6$	1	$3.9 \cdot 10^3$	15
$13.84 \cdot 10^6$	2	$2.2 \cdot 10^3$	16
$10.00 \cdot 10^6$	3	950	17
$6.434 \cdot 10^6$	4	550	18
$4.304 \cdot 10^6$	5	210	19
$2.479 \cdot 10^6$	6	100	20
$1.400 \cdot 10^6$	7	47	21
$0.820 \cdot 10^6$	8	21	22
$0.400 \cdot 10^6$	9	10.0	23
$0.200 \cdot 10^6$	10	4.75	24
$100 \cdot 10^3$	11	2.12	25
$45 \cdot 10^3$	12	1.00	26
$25 \cdot 10^3$	13	0.45	27
$9.5 \cdot 10^3$	14	0.20	28

Table 5. Multiplication factor calculated with homogeneous cross sections

	DYN3D-MG with homogeneous cross sections from SCALE	DYN3D-MG with homogeneous cross sections from SERPENT	SERPENT with continuous energy library	KENO with continuous energy library
K-eff	0.99117	0.99392	0.99189	0.99475
Difference to SERPENT [pcm]	–73	205	–	290
Difference to KENO [pcm]	–363	–84	–290	–
Difference to experimental value [pcm]	–960	–681	–887	–597

The multiplication factor produced by DYN3D-MG is in a good agreement with Monte-Carlo results and experimental values. The difference is around 200 pcm which is better than the results obtained with homogeneous cross section.

5.2 Radial reaction rates

During BFS-62-3A experiment the reaction rates for ^{235}U, ^{238}U and ^{239}Pu were measured. Chambers with fission materials are placed in the inter-tube clearance of the core. Radial reaction rates (measured points are in the mid-plane of the core) were calculated with DYN3D-MG using different cross section sets. As far as a homogeneous model is used, the calculated reaction rates are averaged according to the DYN3D-MG calculation mesh size. Both calculated and measured values are normalized to the value of the center point (R = 0).

The results obtained (see Fig. 5) for ^{235}U appears to be more consistent with measured values. The comparisons of ^{238}U and ^{239}Pu reaction rates show greater deviation. This

Table 6. Multiplication factor calculated with homogenized weighted cross sections

	DYN3D-MG with homogenized weighted cross sections from SCALE	KENO with continuous energy library	SERPENT with continuous energy library
K-eff	0.999596	1.00146	0.999688
Difference to SERPENT [pcm]	–186	–	–177
Difference to KENO [pcm]	–9	177	–
Difference to experimental value [pcm]	–110	75	–101

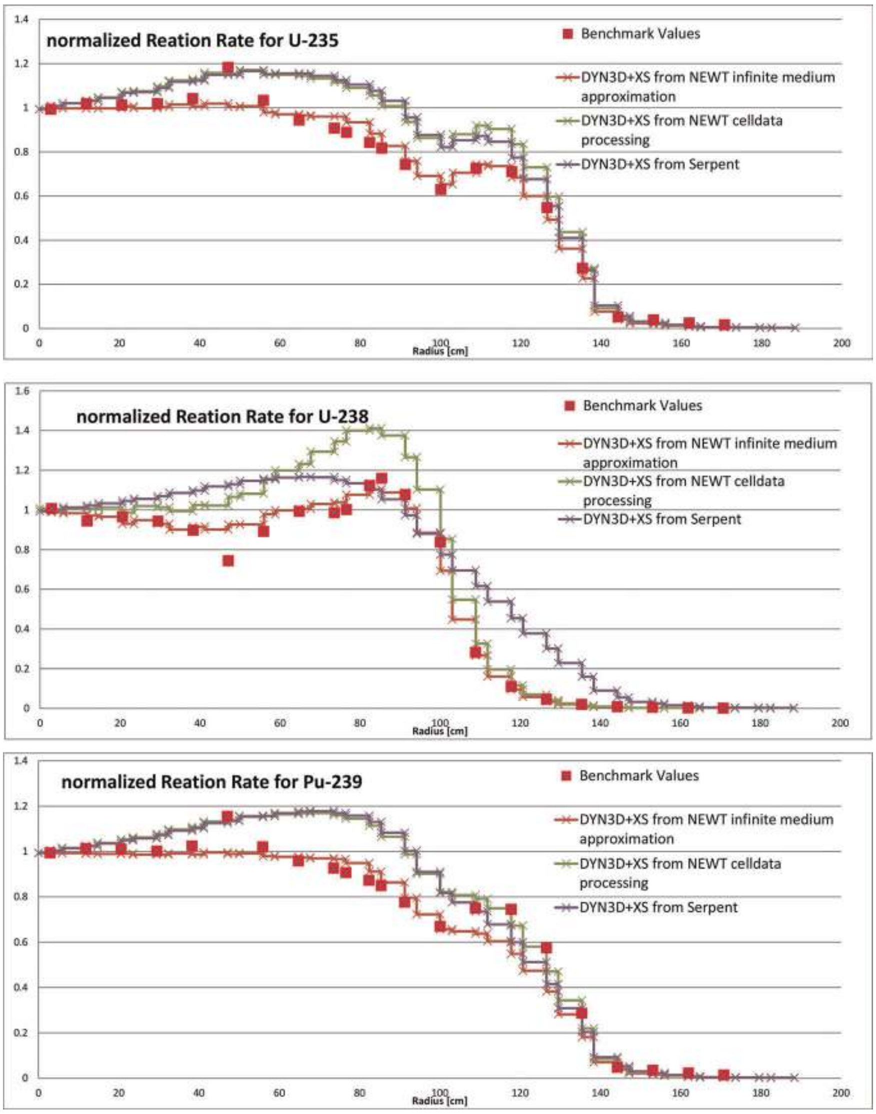

Fig. 5. Radial reaction rates

may be affected either by cross section treatment above 1 MeV or by DYN3D-MG calculation mesh size. The results from DYN3D-MG with homogeneous cross sections generated with NEWT are closer to the measured values. The results calculated with homogenized weighted cross sections and homogeneous cross sections calculate with SERPENT are close to each other. All performed calculations failed to predict the flux depression for the safety rod mock-up located at about 45 cm from the center of the core. Overall the comparisons of the results show that the spatial flux distribution needs further detailed investigations in order to understand the discrepancies.

5.3 Sodium Void Reactivity Effect

The SVRE was calculated in the same way as for heterogeneous model. Homogenized sodium voided IC, MC, OC and MOX fuel elements were used for the case of voided core. SVRE is calculated with DYN3D-MG using the homogeneous cross sections and homogenized weighted cross sections from NEWT (SCALE). The Table 7 shows the results obtained.

5.4 Control Rod and Safety Rod weight

The weights of different control rod and safety rod are calculated with DYN3D-MG with same cross section sets as for SVRE (see Table 8). The accuracy of the calculation is compatible with Monte-Carlo calculations.

6 Conclusion

Monte-Carlo simulations of BFS-62-3A critical experiment with KENO (SCALE6.0) and SERPENT codes with ENDF/B-VII.0 continuous energy library show good agreement with measured values and reference codes simulations. SCALE and SERPENT continuous energy libraries, based on ENDF/B 7.0 evaluated data, are suited for reference calculations. A simplified model was applied to validate the deterministic method on the example of DYN3D code. The few-group macroscopic cross sections were prepared using SCALE (238 group library) and SERPENT (continuous energy cross section libraries). The overall effect of model simplification appears to be dependent on few-group cross section processing. Apparently, the simple cross section homogenization is not accurate enough. Critical calculations with DYN3D-MG showed that corrected homogenized macroscopic cross sections can significantly improve results. In the case of SVRE, reaction rates and other neutronic parameters sensitive to spatial effects calculations an additional corrections in cross sections are required.

Benchmark calculations with DYN3D-MG proved that it capable to perform fast spectrum system critical analysis. Since this code is considered to be used in coupled version with thermo-hydraulic code ATHLET for transient calculations, spatial flux distribution need to be additional studied.

(Received on 1 March 2016)

References

1 *NEA/NSC/DOE* 1 BFS2-LMFR-EXP-001 CRIT-SPEC-REAC-RRATE. BFS-62-3A Experiment: Fast Reactor Core with U and U-PU of 17 % Enrichment and Partial Stainless Steel Reflector. (2006)
2 *SCALE*: A Modular Code System for Performing Standardized Computer Analyses for Licensing Evaluation. NUREG/CR-0200, ORNL/NUREG/CSD-2/R5, Oak Ridge, January 1997
3 *Leppänen J.*: Serpent – a Continuous-Energy Monte Carlo Reactor Physics Burnup Calculation Code. 2013

Table 7. SVRE DYN3D-MG calculation results [pcm]

	DYN3D-MG with homogeneous cross sections from SCALE	DYN3D with Homogenized weighted cross sections from SCALE	Experiment
Inner core	–15	–31	–57 ± 3
Middle core	–4	–21	–15 ± 2
Outer core	–29	–68	–32 ± 2
MOX core	–19	–37	–71 ± 3

Table 8. Control and safety rods weights calculated with DYN3D code

Rod type	DYN3D-MG with homogeneous cross sections from SCALE		DYN3D-MG with Homogenized weighted cross sections from SCALE	
	Calculated value, pcm	Difference with experimental value, pcm	Calculated value, pcm	Difference with experimental value, pcm
SR-2-2(a)	–645	53	–322	–270
SR-2-5(a)	–633	86	–501	–46
CR-1-3	–401	60	–339	–2
CR-1-6	–380	39	–462	121
CR-3-5	–358	73	–282	–4
CR-3-11	–328	46	–423	141

4 *Grundman, U.; Rohde, U.; Mittag, S.; Kliem, S.*: DYN3D Code for Calculation of Transience in Light Water Reactors (LWR) with Hexagonal or Quadratic Fuel Elements
5 *Rearden, B. T.*: Verification Methods for the SCALE Code System. Proc. Verification and Validation for Nuclear Systems Analysis Workshop II, North Myrtle Beach, SC, May 24–28, 2010
6 *Efimov, E. F.; Kochetkov, A. L.*: Experimental Investigation of BFS-62-3 Critical Assemblies. Preprint IPPE, 2853 (2000) (in Russian)
7 *Marinoni, A.; Girardin, G.; Mikityuk, K.*: Analysis of the BN-600 fast-spectrum core mock-up at BFS-2 zero-power facility using MCNPX. Annals of Nuclear Energy 44 (2012) 26–33, DOI:10.1016/j.anucene.2012.01.011
8 *IAEA*: BN-600 Hybrid Core Benchmark Analyses, Results from a Coordinated Research Project on Updated Codes and Methods to Reduce the Calculational Uncertainties of the LMFR Reactivity Effects. IAEA-TECDOC-1623, 2010
9 *Manturov G. N.; Nikolayev M. N.; Tsiboulia A. M.*: Code for Constants Preparation CONSYST. Preprint IPPE, 2828 (2000), (in Russian)
10 *Waltar, A. E., Todd, D. R., Tsvetkov, P. V.*: Fast spectrum reactors, Springer-Verlag, 2012, DOI:10.1007/978-1-4419-9572-8
11 *Fridman, E.; Shwageraus, E.*: Modeling of SFR cores with Serpent–DYN3D codes sequence. Annals of Nuclear Energy 53 (2013), DOI:10.1016/j.anucene.2012.08.006

The authors of this contribution

Vladimir Ivanov
Scientific and Engineering Centre for Nuclear and Radiation Safety (SEC NRS)
Malaya Krasnoselskayast/2/8, bld. 5
107140 Moscow, Russian Federation

Jeremy Bousquet (corresponding author)
E-mail: jeremy.bousquet@grs.de
Gesellschaft für Anlagen- und Reaktorsicherheit gGmbH (GRS)
Forschungszentrum
Boltzmannstraße 14
85748 Garching bei München
Germany

Bibliography
DOI 10.3139/124.110730
KERNTECHNIK
81 (2016) 5; page 512–519

ISSN 0932-3902

Books · Bücher

Ageing Management of Concrete Structures in Nuclear Power Plants. IAEA Nuclear Energy Series No. NP-T-3.5, Published by the International Atomic Energy Agency, 2016, ISBN 978-92-0-102914-0, 211 pp., 55.00 EUR.

This publication is one in a series of reports on the assessment and management of ageing of major nuclear power plant components. Current practices for assessment of safety margins (fitness for service) and inspection, monitoring and mitigation of ageing related degradation of selected concrete structures related to NPPs are documented. Implications for and differences in new reactor designs are discussed. This information is intended to help all involved directly and indirectly in ensuring the safe operation of NPPs, and also to provide a common technical basis for dialogue between plant operators and regulators when dealing with age related licensing issues.

This publication provides information regarding good practices for assessment and management of ageing related to concrete structures within an NPP. It supersedes IAEA-TECDOC-1025, Assessment and Management of Ageing of Major Nuclear Power Plant Components Important to Safety: Concrete Containment Buildings, which was published in 1998. Significant ageing related events have occurred since then that could impact future plant operation, such as alkali–silica reactivity in concrete, delamination events, larger than anticipated loss of prestressing force, SFP leakage, corrosion of steel in water intake structures, etc. These events led to new ageing management actions by both NPP operators and regulators.

Specifically, this publication includes:

(a) State of the art information regarding ageing management of concrete structures in NPPs throughout their entire service life;
(b) Background material indicating the importance of AMPs;
(c) Current practices and techniques for assessing fitness for service and for inspection, monitoring and mitigation of ageing related degradation of CCBs and other concrete structures important to the safe and reliable operation of NPPs;
(d) A technical basis for developing and implementing a systematic AMP;
(e) Guidelines to help ensure ageing management is taken into account during different NPP lifecycle phases, that is, design, fabrication, construction, commissioning, operation (including long term operation and extended shutdown) and decommissioning;
(f) Research material related to ageing and lessons learned.

Section 2 introduces the generic AMP as it relates to concrete structures. Section 3 describes where concrete is used in NPPs. The process of an effective AMP is described in Sections 4–8, and includes the following:

(a) Understanding ageing (Section 4);
(b) Developing and optimizing the AMP (Section 5);
(c) Plant operation (Section 6);
(d) Inspection, monitoring and assessment of structures (Section 7);
(e) Maintenance and repair of ageing effects (Section 8).

Each section includes steps in the process for the development of an AMP and information specific to concrete structures, which supplements the generic information provided in IAEA publication NS-G-2.12. Section 9 summarizes the conclusions of this publication. The appendices cover IAEA activities on ageing management (Appendix I), describe containment structures (Appendix II) and ageing management practices and operating experience in selected Member States (Appendices III and IV), describe ageing management practices in non-nuclear industries (Appendix V) and provide details of the coordinated research project (CRP) conducted in the 1990s (Appendix VI) and case studies and example applications of modelling of concrete structures (Appendix VII).